

Sliding Mode Control via Fuzzy Multi-Level Switching control scheme for DFIG based WECS

S. LABDAI¹, N. BOUNAR², A. BOULKROUNE², and B. HEMICI¹

¹LCP, Ecole Nationale Polytechnique (ENP), 10, Av. Hassen Badi, BP182, Algiers, Algeria.

²LAJ, University of Jijel, BP98, Ouled Aissa, Jijel, Algeria

E-mails: sami.labdai@gmail.com, bounar18@yahoo.fr,
boulkroune2002@yahoo.fr, bhemici@yahoo.fr

Abstract. This paper presents a new *sliding mode control* (SMC) via *fuzzy multi-level switching* (FMLS) technique for *doubly fed induction generator-based wind energy conversion system* (DFIG-based WECS). The main objectives are: 1) extraction of maximum power from the wind by achieving *maximal power point tracking* (MPPT) strategy, and 2) supplying the grid with zero reactive power. The SMC is combined with FMLS control to minimize the undesirable effect of chattering inherent to the conventional SMC. Based on the measured error, five error levels are selected extra-small, small, middle, large, and extra-large. For each error level there is different switching level. The DFIG and MLS controller will be tested against various perturbations. Simulation results using Simulink/Matlab conclude that the proposed controller succeeded in eliminating perturbation and minimizing the chattering effect.

Key-words: Wind energy conversion system, MPPT, DFIG, Sliding mode control, Fuzzy control, Multi-level switching.

Nomenclature

WT	Wind turbine	J	Turbine total inertia ($Kg m^2$)
DFIG	Doubly fed induction generator	f	Turbine total external damping (Nm/rad s)
MPPT	Maximum power point tracking	Ω	Generator speed (rad/s)
d, q	Synchronous reference frame index	ω, ω_s	Angular speed, synchronous speed (rad/s)
s, r	Stator and rotor indices	G_b	Gearbox coefficient
V	Wind speed (m/s)	v, i	Voltage (V), current (A)
ρ	Air density (kg/m^3)	φ, T_{em}	Flux (Wb), Electromagnetic torque (Nm)
R_b	Blades length (m)	P, Q	Active power (W), reactive power (VAR)
T_a	Aerodynamic torque (Nm)	p	Number of poles pairs
P_a	Aerodynamic power (W)	L, M	Inductance, mutual inductance (H)
C_p	Power coefficient	R	Resistance (Ω)
Ω_t	Wind turbine rotor speed (rad/s)	σ	Leakage flux coefficient ($\sigma = 1 - M^2/L_s L_r$)

1. Introduction

Nowadays, wind energy has become the most promising renewable energy source [1, 2]. The exploitation of wind energy is growing for the reason that it is a clean source and harmful to nature. The so-called *doubly-fed induction generator* (DFIG) is widely used in wind energy conversion system [1]. For the variable speed wind energy conversion applications, The DFIG rotor windings are connected to the line-grid via a bi-directional power converter, and the stator is directly connected to the line-grid. Compared with other configurations such as fixed-speed asynchronous induction generator or variable-speed synchronous generator with full-power stator converter, the DFIG-based WECS has many advantages: 1) In variable speed operation, the asynchronous nature of the DFIG allows to generate stator constant-frequency power, while the extracted wind power can be optimized, as the shaft speed can be adjusted proportionally to the wind speed. 2) Possibility to operate at sub-and super-synchronous modes. 3) The rotor power converter rating is reduced to handle a small fraction (30%) of the total converted power [3, 4]. However, it is a challenge to control the DFIG-based WECS since it presents a multivariable nonlinear and coupled system with many parameter uncertainties (resistance, inductance, inertia, friction coefficient).

Many proposed control schemes for DFIG-based WECS can be found in literature, most of them are based on the work presented in [7], authors used vector control with linear *proportional integral* (PI) controllers to achieve a decoupled control of the active and reactive power. However, with the linear control techniques, the system robustness against parameter variations cannot be guaranteed. To overcome this difficulty, Different robust nonlinear strategies have been presented in the literature, among the most popular: nonlinear adaptive control strategy which was proposed in [8, 9]. Using Lyapunov approach, the robustness condition is guaranteed only to constant unknown parameters. In [10] a robust backstepping control for the DFIG has been proposed. The controlled system has to have a specific triangular form.

In recent years, the *sliding mode control*(SMC) has gained a lot of attention. It is popular for robust control of nonlinear systems. This controller' s structure which is based on a discontinuous term added to the sliding surface is able to eliminate not only external perturbation but also achieves robustness against parameters variation and uncertainties. In [11, 12], SMC has been proposed to control the DFIG-based WECS. Simulation results show that SMC of the DFIG-based WECS is able to track the desired active and reactive power with good system robustness and high tracking performances. But, discontinuous term gain is chosen big enough to eliminate the upper bound of uncertainties, unfortunately, this leads to the undesirable phenomenon of chattering and its effect on stressing and damaging the DFIG. Researchers developed many various technique based on smoothing the discontinuous term. We can cite the adaptive sliding mode control [13], and the high order sliding mode control [14, 15]. These solutions prove effective in reducing the chattering and guarantying the system robustness, but tend to slow the system responses. In [16], a new method called multi-level switching technique has been proposed. This approach use variable switching gains to eliminate the chattering effect. The combination of Fuzzy logic and SMC has been studied in [17] and [18]. It gives the possibility to implement human thinking in control strategy and it was able to achieve the system robustness with less chattering effect.

This paper presents a new *sliding mode control* (SMC) via *fuzzy multi-level switching* (FMLS) technique for DFIG-based WECS. The controller guarantees the maximization of the captured power and null reactive power regulation. The fuzzy system is used to find the optimal switching gain for the sliding mode controller that ensures both the system robustness and the chattering

free operation.

2. Description of the DFIG-based WECS

Figure 1 presents a DFIG based WECS. The turbine converts wind power to mechanical power, the DFIG speed is then the turbine speed multiplied via the gear box, finally the DFIG supplies the grid directly with electrical power.

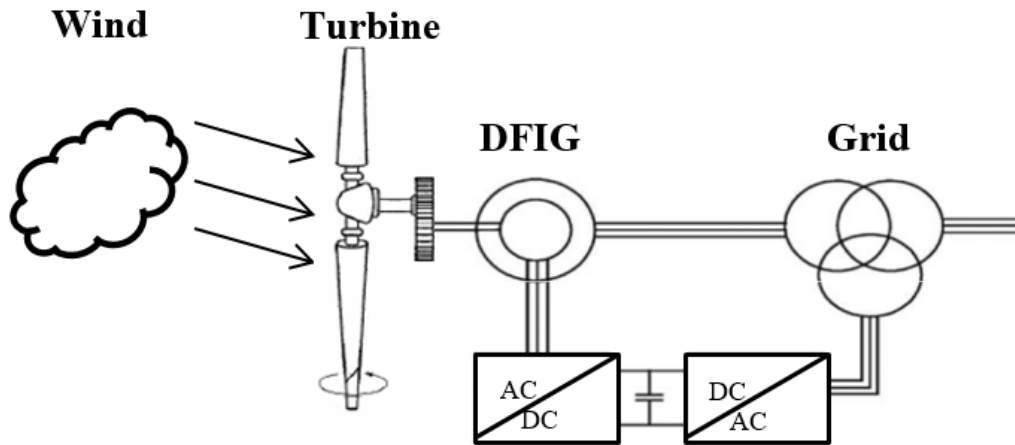


Fig. 1. DFIG-based WECS.

2.1. Turbine model

The wind kinetic power is directly proportional of wind speed and is given by:

$$P_a = \frac{1}{2} \rho S C_p(\lambda, \beta) V^3 \quad (1)$$

where V is the wind speed, ρ is the air density 1.225 kg/m^3 , S is the area circulated by turbine blades, and C_p the power conversion efficiency.

The relation giving the relation between rotor aerodynamic torque T_a , turbine speed Ω_t , and aerodynamic power P_a , is given by :

$$T_a = \frac{P_a}{\Omega_t} = \frac{1}{2\Omega_t} \rho S C_p(\lambda, \beta) V^3 \quad (2)$$

The power coefficient $C_p(\lambda, \beta)$ is a function of the blade pitch angle β , as well as the tip-speed ratio λ . It is a function of V the wind speed, Ω_t the turbine speed, and R the blade diameter.

$$\lambda = \frac{R_b \Omega_t}{V} \quad (3)$$

we consider a fixed pitch angle and controlling achieving the maximum power coefficient by achieving optimal tip speed ratio λ . The power coefficient as a function of λ and $\beta=0$ is shown in figure 2

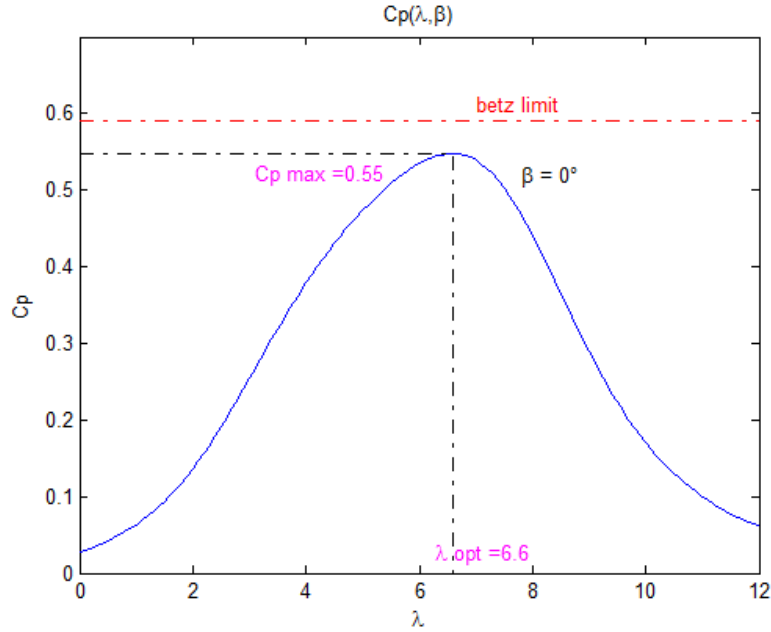


Fig. 2. Power coefficient.

2.2. DFIG model

The DFIG stator is connected directly to the line grid and the rotor connected via converter to the line grid. The DFIG model presented after park transformation to rotating frame dq :

Stator and rotor electrical equations are given by:

$$\begin{cases} v_{ds} = R_s i_{ds} + \frac{d}{dt} \Phi_{ds} - \omega_s \cdot \Phi_{qs} \\ v_{qs} = R_s i_{qs} + \frac{d}{dt} \Phi_{qs} + \omega_s \cdot \Phi_{ds} \\ v_{dr} = R_r i_{dr} + \frac{d}{dt} \Phi_{dr} - \omega_r \cdot \Phi_{qr} \\ v_{qr} = R_r i_{qr} + \frac{d}{dt} \Phi_{qr} + \omega_r \cdot \Phi_{dr} \end{cases} \quad (4)$$

with $v_{s(r)}$ is the stator(rotor) voltage, $i_{s(r)}$ is the stator(rotor) current, $\Phi_{s(r)}$ is the stator(rotor) flux, $R_{s(r)}$ is stator(rotor) resistance, $\omega_{s(r)}$ is stator(rotor) angular speed.

Stator and rotor flux equations are given by:

$$\begin{cases} \Phi_{ds} = L_s \cdot i_{ds} + M \cdot I_{dr} \\ \Phi_{qs} = L_s \cdot i_{qs} + M \cdot I_{qr} \\ \Phi_{dr} = L_r \cdot i_{dr} + M \cdot I_{ds} \\ \Phi_{qr} = L_r \cdot i_{qr} + M \cdot I_{qs} \end{cases} \quad (5)$$

with M , $L_{s(r)}$ is the mutual, stator(rotor) inductance.
The DFIG electromagnetic torque is given by:

$$T_{em} = p \frac{M}{L_s} (\Phi_{qs} i_{dr} - \Phi_{ds} i_{qr}) \quad (6)$$

where p is the number of pole pairs.

The mechanical equation of the DFIG-based WT is given by:

$$J \frac{d\Omega}{dt} = T_a - T_{em} - f\Omega \quad (7)$$

where J turbine total inertia, Ω is the DFIG speed, T_{em} is the generator electromagnetic torque and f is the damping coefficient .

3. Control strategy

3.1. Maximum power point tracking MPPT

Variable speed WECS have the flexibility to operate under various speeds independent of wind speed, but for a fixed wind speed there is only one DFIG speed that products maximum power.

$$\Omega_{opt} = \frac{\lambda_{opt} V}{R_b} \quad (8)$$

The DFIG speed dynamic equation given in (7) and by putting $e_v = T_a$ as external perturbation, it can be written as:

$$\frac{d\Omega}{dt} = \frac{1}{J} (-T_{em} - f\Omega + e_v) \quad (9)$$

It is a first order differential equation, by considering T_{em} the input and Ω the output, designing a PI controller can track the reference Ω_{opt} .

3.2. Vector control

The vector control principle depends on linking the stator flux to the d-axis of the frame so we have:

$$\Phi_{qs} = 0, \Phi_{ds} = \Phi_s \quad (10)$$

Replacing (10) in (6) the electromagnetic torque equation becomes linear and proportional to the rotor current i_{qr} .

$$T_{em} = \frac{PM}{L_s} (\Phi_s i_{qr}) \quad (11)$$

From (9), knowing that T_{em} is the electromagnetic torque needed to reference tracking of Ω_{opt} , and considering (11) we obtain $i_{qr.ref}$ needed to reference tracking of Ω_{opt} , and it is given by:

$$i_{qr.ref} = \frac{L_s}{PM\phi_s}(T_{em.ref}) \quad (12)$$

The stator active and reactive power is given by:

$$\begin{cases} P_s = (v_{ds}i_{ds} + v_{qs}i_{qs}) \\ Q_s = (v_{qs}i_{ds} - v_{ds}i_{qs}) \end{cases} \quad (13)$$

From on (10), considering a stable grid and the by neglecting the stator resistance we get:

$$\begin{cases} v_{ds} = 0 \\ v_{qs} = v_s = \omega_s \phi_{ds} \end{cases} \quad (14)$$

Replacing (10) in (4) the stator currents are:

$$\begin{cases} i_{ds} = -\frac{M}{L_s}i_{dr} + \frac{\phi_s}{L_s} \\ i_{qs} = -\frac{M}{L_s}i_{qr} \end{cases} \quad (15)$$

Replacing (10), (14), and (15) in (13) the stator reactive power can be written as:

$$Q_s = \left(\frac{v_{qs} \cdot \phi_{ds}}{L_s} - \frac{M}{L_s} v_{qs} i_{dr} \right) \quad (16)$$

To meet the grid requirement (null reactive power), we can write:

$$0 = \frac{v_{qs} \cdot \phi_{ds}}{L_s} - \frac{v_{qs} \cdot M i_{dr}}{L_s} \quad (17)$$

From (17), the rotor current reference $i_{dr.ref}$ is:

$$i_{dr.ref} = \frac{\phi_{ds}}{M} \quad (18)$$

We can resume the DFIG-based WECS control objectives in Table 1.

Table 1. Control objectives

Commands	Objectives
$i_{dr} = i_{dr.ref}$	$Q_s = 0$
$i_{qr} = i_{qr.ref}$ means to $T_{em} = T_{em.ref}$	$\Omega = \Omega_{opt}$ means to $\lambda = \lambda_{opt}$

3.3. Sliding mode control of the DFIG-based WECS

From (4) and the above simplifications, the DFIG electrical reduced model is:

$$\begin{cases} \frac{di_{dr}}{dt} = f_1 + \delta_1 + gv_{dr} \\ \frac{di_{qr}}{dt} = f_2 + \delta_2 + gv_{qr} \end{cases} \quad (19)$$

where: $f_1 = -R_r i_{dr} + L_r \cdot (\omega_s - \omega) \sigma i_{qr}$, $f_2 = -R_r i_{qr} + L_r (\omega_s - \omega) \sigma i_{dr} - \frac{M}{L_r} (\omega_s - \omega) \phi_{ds}$, $g = \frac{1}{L_r \sigma}$, $\delta_j(x)$ for $j = 1, 2$ represent bounded uncertainties, ω_s is the stator angular speed $\omega_s = 2\pi f$,

and f is the grid frequency; ω is the rotor angular speed $\omega = P\Omega$, and σ is the leakage coefficient $\sigma = 1 - \frac{M^2}{L_s L_r}$

In this section we present the classical sliding mode, it is simply based on four steps:

3.3.1. Choice of surface

To achieve tracking of the rotor currents we choose the error to be the sliding surface:

$$\begin{cases} S_1 = e_{dr} = i_{dr} - i_{dr.ref} \\ S_2 = e_{qr} = i_{qr} - i_{qr.ref} \end{cases} \quad (20)$$

3.3.2. Choice of Lyapunov function

The Lyapunov candidate function is chosen as:

$$V_j = \frac{1}{2} S_j^2, j = 1, 2 \quad (21)$$

The time derivative of this function is:

$$\dot{V}_j = S_j \dot{S}_j, j = 1, 2 \quad (22)$$

By deriving (20) we have

$$\dot{S}_j = F_j(x) + \delta_j(x) + g u_j, j = 1, 2 \quad (23)$$

where $F_1 = f_1 - \frac{di_{dr.ref}}{dt}$, $F_2 = f_2 - \frac{di_{qr.ref}}{dt}$, $u_1 = v_{dr}$, $u_2 = v_{qr}$

Replacing (23) in (22), the Lyapunov function derivative is:

$$\dot{V}_j = S_j (F_j(x) + \delta_j(x) + g u_j), j = 1, 2 \quad (24)$$

3.3.3. Control law structure

The SMC control law is:

$$u_j = u_{j,eq} + u_{j,d}, j = 1, 2 \quad (25)$$

$$\begin{cases} u_{j,eq} = \frac{1}{g} (-F_j(x) - k_j S_j) \\ u_{j,d} = \frac{1}{g} (-\lambda_j \text{sign}(S_j)) \end{cases}, j = 1, 2 \quad (26)$$

where: $u_{j,eq}$ is the equivalent control term, $u_{j,d}$ is the discontinuous term k_j and λ_j (for $j = 1, 2$) are positive constants.

3.3.4. Stability proof of the closed loop system with SMC

As long as $g \neq 0$ the control law given in (25) is finite and by replacing it in (24) for $j=1,2$ we obtain:

$$\dot{V}_j = -k_j S_j^2 + S_j(\delta_j(x) - \lambda_j \text{sign}(S_j)) \quad (27)$$

$$\dot{V}_j \leq -k_j S_j^2 + |S_j|(|\delta_j(x)| - \lambda_j) \quad (28)$$

Assuming that $k_j > 0$ and that $|\delta_j(x)| < \lambda_j$, from the Barbalet lemma, we conclude that the SMC controller given guarantees the system asymptotic convergence and robustness against uncertainties produced by external perturbation and internal parameters variations.

3.4. Fuzzy sliding mode control of the DFIG-based WECS

One main advantage of SMC is his robustness against internal and external disturbances. Unfortunately, the SMC main drawback is the undesirable chattering phenomenon always occurs in the sliding and steady state modes as high frequency oscillations, it's origin is the discontinues term in the SMC control law. Therefore, a *Fuzzy sliding mode control* (FSMC) system, in which a fuzzy logic inference mechanism is used to mimic the switching control law.

Design of the Fuzzy sliding mode control

Let define the sliding surface S_j as the input linguistic variables of a fuzzy system, and the fuzzy switching control term $u_{j,d} = \lambda_j \text{sign}(S_j)$ as its output. Then, the associated fuzzy linguistic rule base can be summarized as follows.

The proposed fuzzy sliding mode controllers in [18], it depends on seven linguistic variables NB, NM, NS, EZ, PS, PM, PB, triangular membership functions are chosen to represent the linguistic variables and fuzzy singletons for the outputs are used. as shown in figure 3, and table 2.

where: NB: Negative Big, - NM: Negative Middle, - NS: Negative Small, - EZ: Equal Zero, - PS: Positive Small, - PM: Positive Middle, - PB: Positive Big.

Table 2. Base of rules for FSMC

S_j	NB	NM	NS	EZ	PS	PM	PB
NB	NB	NB	NB	NB	NM	NS	EZ
NM	NB	NB	NB	NM	NS	EZ	PS
NS	NB	NB	NM	NS	EZ	PS	PM
EZ	NB	NM	NS	EZ	PS	PM	PB
PS	NM	NS	EZ	PS	PM	PB	PB
PM	NS	EZ	PS	PM	PB	PB	PB
PB	EZ	PS	PM	PB	PB	PB	PB

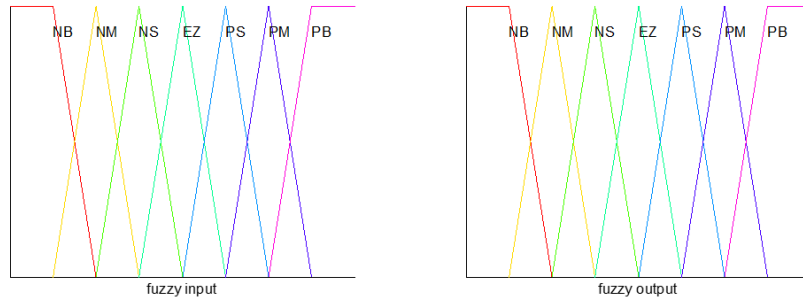


Fig. 3. Input and output membership functions of the fuzzy system.

The *fuzzy sliding mode controller* (FSMC) is a modification of the sliding mode controller, where the switching controller $u_{j,d}$ has been replaced by a fuzzy control input as given below

$$u_j = u_{j,eq} + u_{j,fuzzy}, j = 1, 2 \tag{29}$$

3.5. Fuzzy multi-level switching technique control of the DFIG-based WECS

The discontinuous term gain has to be greater than the upper bound of uncertainties. In classical SMC before constructing the control law, the upper bound is prior fixed and remains unchangeable during the control process.

$$\begin{cases} \lambda_j > \bar{\Delta}_j \\ \bar{\Delta}_j = \sup\{|\delta_j(x)|, \forall x\} \end{cases} \tag{30}$$

But, discontinuous term gain is chosen big enough to eliminate the upper bound of uncertainties, unfortunately, this leads to the undesirable phenomenon of chattering and its effect on stressing and damaging the DFIG. In Fuzzy Multi-Level Switching we consider an unknown upper bound directly linked to the tracking error, if the error is big the switching command gain is great to guarantee the robustness, the more it is reduced the more the gain is small enough to keep the robustness and reduce the chattering effect, the fuzzy system is presented in figure 4 and table 3.

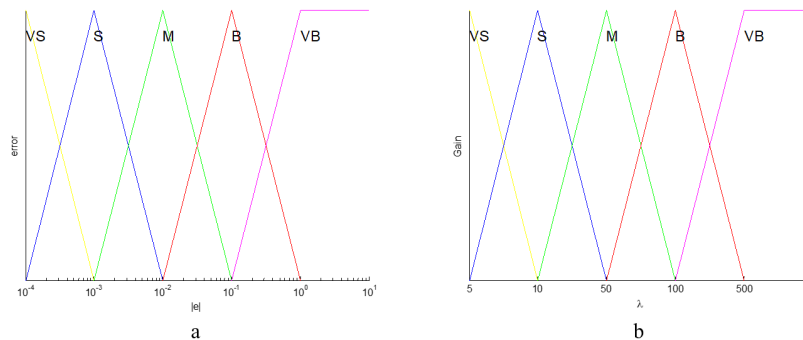


Fig. 4. a)Input membership function b)Output membership function.

Figure 4.a presents the input variable the absolute value of tracking error $|e_j|, j = 1, 2$.

Where each of the input variables is triangular membership function, fuzzy label of VS: very small, S:small, M: medium, B: big, VB: very big.

Figure 4.b presents the output variable the switching control gain $\lambda_j, j = 1, 2$.

Where each of the output variables is triangular membership function, fuzzy label of VS: very small effort, S:small effort, M: medium effort, B: big effort, VB: very big effort. Table 3 presents the associated fuzzy linguistic rule base

Table 3. Base of rules for FMLS

Rules	Rule1:	Rule2:	Rule3:	Rule4:	Rule5:
Input	VS error	S error	M error	B error	VB error
Output	VS gain	S gain	M gain	B gain	VB gain

Figure 5 resumes the global control scheme of the DFIG-based WECS using SMC via FMLS technique. As is shows, the MPPT is achieved a cascade regulation, the outer loop is the speed loop controlled by a PI controllers, and the inner loop is the current i_{qr} loop together with the current i_{dr} loop which are controlled by two SMC based FMLS controllers.

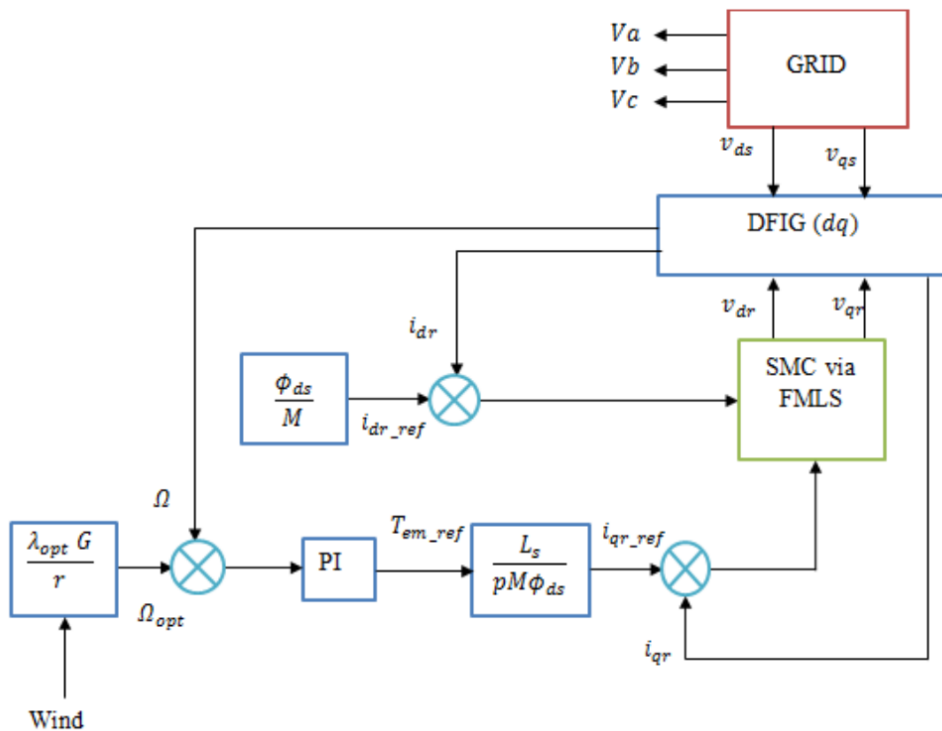


Fig. 5. DFIG based WECS global control scheme.

4. Results and discussion

4.1. Simulation parameters

In order to validate the proposed technique the DFIG based WECS is tested under Simulink/Matlab with the following turbine and DFIG parameters:

Table 4. Simulation parameters

Nominal power P_n	7.5 kW
Stator resistance R_s	0.455 Ω
Rotor resistance R_r	0.62 Ω
Stator inductance L_s	0.084 H
Rotor inductance L_r	0.081 H
Mutual inductance M	0.078 H
Total inertia J	0.3125 Kg.m ²
Poles p	2
Damping f	0.00673 N.m.s/rad
Grid frequency f_n	50 Hz
Nominal speed Ω_n	157 Rad/s

The wind profile used in simulation is presented in figure 6.

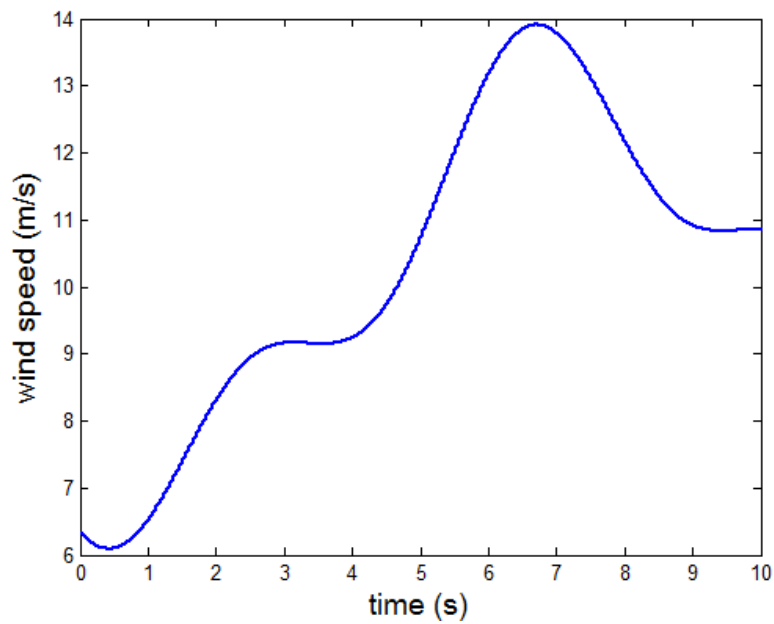


Fig. 6. Wind profile.

The FSMC parameters were not given in [18], and the FSMC gain are selected based on try and fail, $k_1 = k_2 = 100$.

The fuzzy membership functions are based on try and fail, the input membership function which depend on the absolute value of error are given by: $VS=10^{-3}$, $S=10^{-2}$, $M=10^{-1}$, $B=10^0$, $VB=10^1$. The output membership functions are linked to the switching command gain and it is given by: $VS=5$, $S=10$, $M=50$, $B=100$, $VB=500$.

The wind profile is shown in figure 6, it is chosen to simulate real wind speed, it begins in low speed 6m/s and rises to high speed 14 m/s then finally settles to middle speed 10m/s.

To test the robustness of the proposed control scheme, it is compared to normal SMC and the simulation is carried out under the following parametric changes:

- Between 3s-5s : 30% change of the inductance and mutual inductance, and 100% of the rotor resistance.
- Between 5s-7s: 300% change of inertia and Damping coefficient.
- Between 7s-9s : 10% change of network frequency.

4.2. Simulation results

Figures 7–13 show the simulation results of the FSMC and FMLS applied on the DFIG-based WECS.

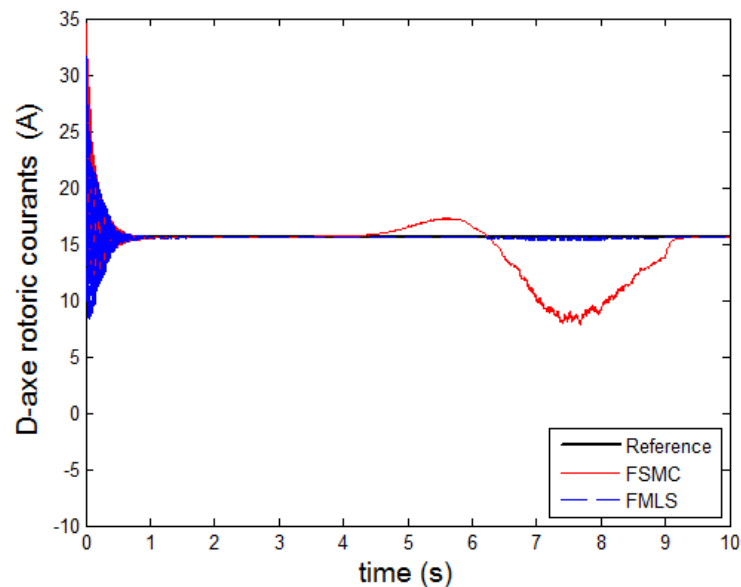


Fig. 7. DFIG rotor current i_{dr} .

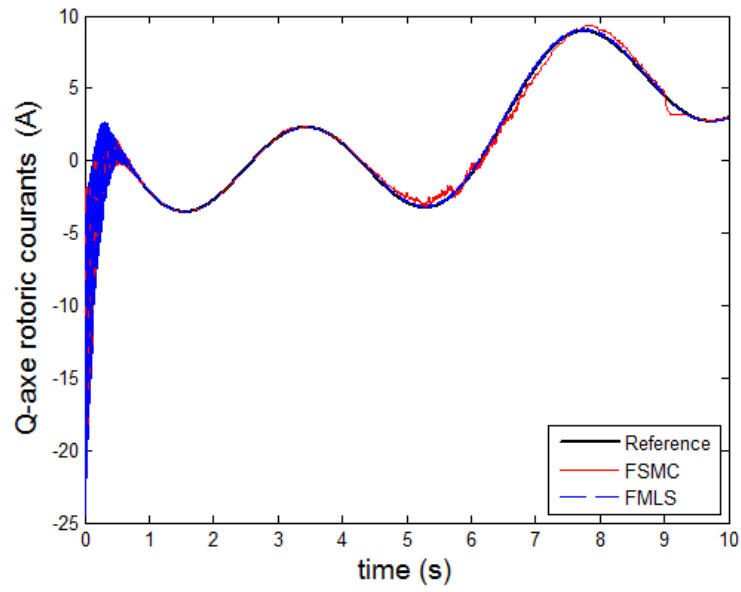


Fig. 8. DFIG rotor current i_{qr} .

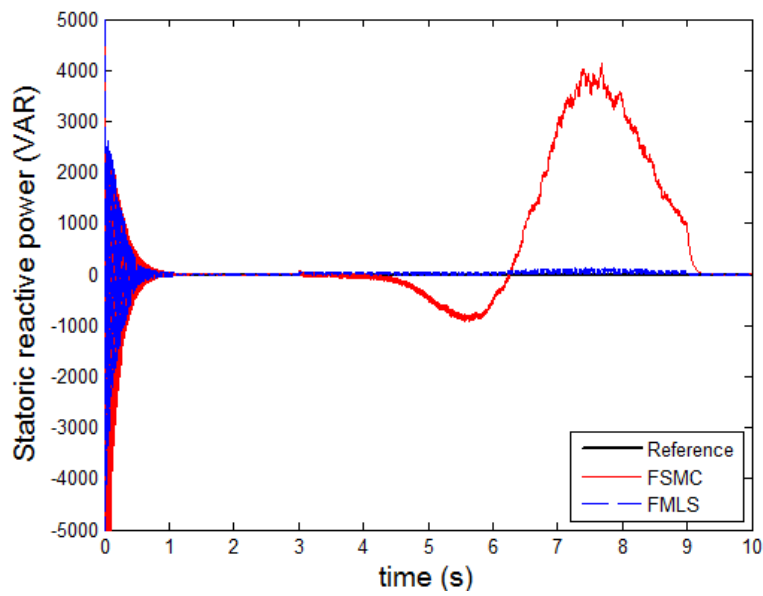


Fig. 9. DFIG stator reactive power.

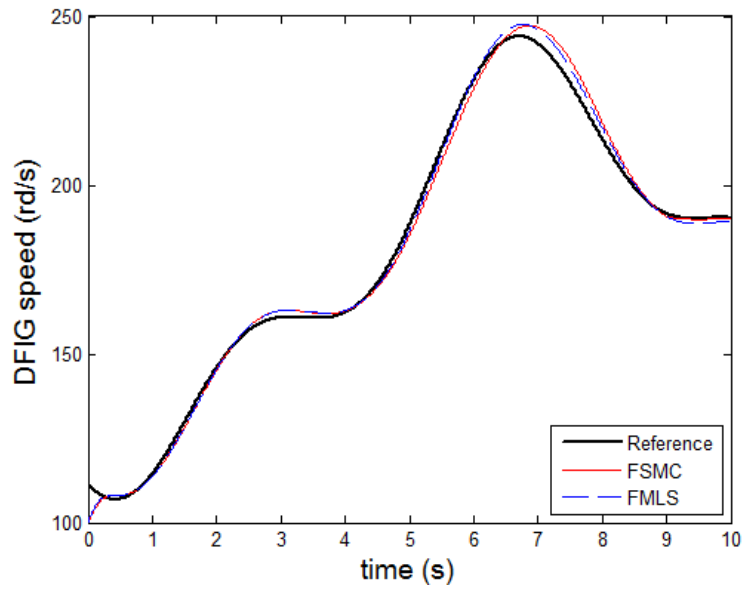


Fig. 10. DFIG speed.

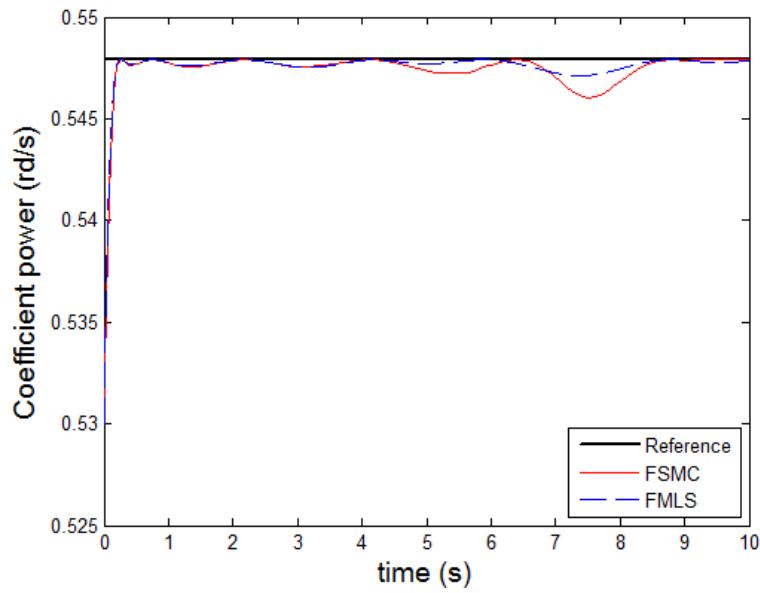


Fig. 11. Turbine power coefficient.

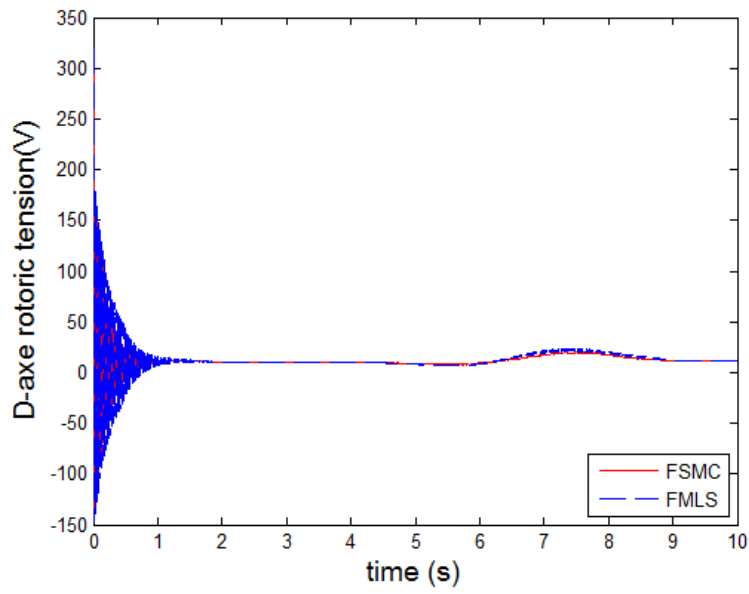


Fig. 12. DFIG rotor voltage v_{dr} .

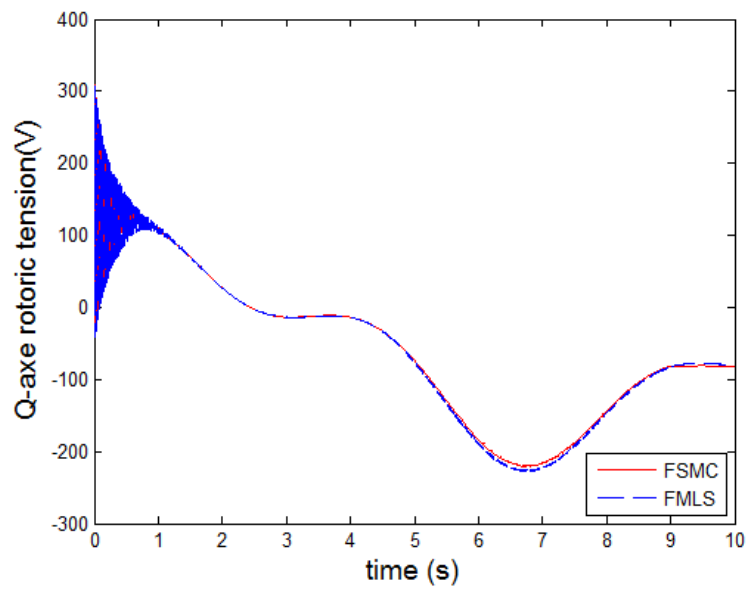


Fig. 13. DFIG rotor voltage v_{qr} .

5. Discussion

Figures (7) and (8) shows the tracking performances of current i_{dr} and i_{qr} , we can see that both control methods have a good robustness, but, The chattering effect in FSMC is much higher. Figures (9), (10), and (11) show the reactive power DFIG speed and power coefficient respectively, the good tracking of these signals means that the proposed approach succeeded in achieving MPPT and producing maximum power with null reactive power injected to the grid. The input control signals (the DFIG voltages v_{dr} and v_{qr}) are shown in figure (12) and (13). For the conventional SMC, the robustness achieved at the price of chattering effect while the proposed controller (SMC via FMLS) guarantees a good robustness against parametric changes with minimized chattering effect, another comparison between the FSMC and the FMLS is presented in table 5. It shows the mean square error of each approach for the speed tracking error currents i_{rd} and i_{rq} tracking error and stator reactive power regulation. We can see the superiority of the proposed fuzzy MLS technic above the fuzzy SMC. One main advantage also with the FMLS the controller calculation time is faster due to the rule reduction in that approach.

Table 5. Comparison of FSMC and FMLS

Approach	$MSE i_{rd}$	$MSE i_{rq}$	$MSE \Omega$	$MSE Q_s$	Calculation time
FSMC	8.2046	7.8291	8.2067	$2.3436 \cdot 10^6$	3.311580 seconds
FMLS	0.74385	0.67452	4.7076	96661	14.121723 seconds

6. Conclusion

In this paper we presented a new FSMC via FMLS control scheme for DFIG-based WECS. The control objectives are extracting the maximum available power from the wind, and supplying the grid with null stator reactive power. The DFIG-based WECS is a perturbed system with many uncertain parameters. To avoid the undesirable phenomenon of chattering in conventional SMC, fuzzy multi-level switching technique is adopted. The discontinuous term of the conventional SMC is calculated according to the absolute value of the tracking error, thus the chattering is minimal and the robustness is not affected. The simulation results compare the performances of the proposed control scheme and the SMC system. The superiority of the SMC via FSMC controller is clearly shown in terms of fast responses, tracking errors under parametric change and the significant chattering reduction.

References

- [1] P. B. ERIKSEN, T. ACKERMANN, H. ABILDGAARD, P. SMITH, W. WINTER, and J. M. RODRIGUEZ GARCIA, *System operation with high wind penetration*, IEEE Power Energy Mag., 2005, pp. 65–74.
- [2] O. ANAYA-LARA, N. JENKINS, J. EKANAYAKE, P. CARTWRIGHT, M. HUGHES, *Wind Energy Generation*, In: Wiley, 2009.
- [3] The US Department of Energy (US DoE), *Wind vision: a new era for wind power in the United States*, online: www.energy.gov/sites/prod/files/wv_chapter4_the_wind_vision_roadmap.pdf
- [4] European Wind Energy Association (EWEA), *Pure power: wind energy targets for 2020 and 2030*, online: www.ewea.org/fileadmin/files/library/publications/reports/Pure_Power_III.pdf

- [5] M. A. POLLER, *Doubly-fed induction machine models for stability assessment of wind farms*, IEEE Power Tech Conference Proceedings, **3**, 2003, Bologna.
- [6] R. DATTA, V. T. RANGANATHAN, *Variable-speed wind power generation using doubly fed wound rotor induction machine—a comparison with alternative schemes*, IEEE Transactions on Energy Conversion **17**, 2002, pp. 414–421.
- [7] R. PENA, J. C. CLARE, G. M. ASHER, *A doubly fed induction generator using back to back converters supplying an isolated load from a variable speed wind turbine*, IEEE Proceeding on Electrical Power Applications **143**, 1996.
- [8] M. BENKAHLA, R. TALEB and Z. BOUDJEMA, *Comparative study of robust control strategies for Dfig based wind turbine*, International Journal of advanced computer science and Applications IIACSA, **7**(2), pp. 455–462, 2016.
- [9] N. BOUNAR, A. BOULKROUNE, F. BOUDJEMA, M, M'SAAD and M. FARZA *Adaptive fuzzy vector control for doubly-fed induction motor*, Neurocomputing **151**, Elsevier, 2015, pp. 756–769.
- [10] S. DRID, M. TADJINE, M. S. NAIT-SAID, *Robust backstepping vector control for the doubly fed induction motor*, IET Control Theory Appl, 2007.
- [11] B. KIRUTHIGA, *Implementation of first order sliding mode control of active and reactive power for DFIG based wind turbine*, International Journal of Informative and futuristic Research, **2**(8), 2015, pp. 2487–2497.
- [12] A. MECHTER, K. KEMIH and M. GHANES, *Sliding mode control of wind turbine with exponential reaching law*, Acta Polytechnic Hungarica, **12**(3), 2015, pp. 167–183.
- [13] N. BOUNAR, F. BOUDJEMA, N. OUCIEF, *Adaptive sliding mode control for double-fed induction machine*, EMP, Algeria, 2011.
- [14] B. BELTRAN *et al.* , *Second-order sliding mode control of a doubly fed induction generator driven wind turbine*, IEEE Transactions on Energy Conversion, **27**(2), 2012 , pp. 261–269.
- [15] C.A EVANGELISTA, F. Valenciaga and P. Puleston, *Multivariable 2-sliding mode control for wind energy conversion system based on a doubly-fed induction generator*, International Journal of Hydrogen Energy, **37**, 2012, pp. 10070–10075.
- [16] S. SUTHA, P. LAKSHMI, S. SANKARANARAYANAN, H. A. SHABEER, *Improved robustness and finite time convergence for a multivariable process using integral terminal sliding mode controller via multi-level switching*, Journal of scientific and industrial research, **74**, 2015, pp. 444–449.
- [17] R. J. WAI, *Fuzzy sliding-Mode control using adaptive tuning technique*, IEEE transactions on industrial electronics, **54**(1), 2007.
- [18] Z. BOUDJEMA, A. MEROUFEL, Y. DJERRIRI, E. BOUNADJA, *Fuzzy sliding mode control of a doubly fed induction generator for wind energy conversion*, Carpathian Journal of Electronic and Computer Engineering, **6**(2), 2013, pp. 7–14.

M. SAMI LABDAI: was born in Taher, Jijel, Algeria. He received the master degree in automatics and industrial informatics from the university of Jijel in 2014. Currently he is an automatics PHD student in National Polytechnic School (ENP) of Algiers, Algeria. His research interests include: renewable energy, electrical drives, robust control, fuzzy logic, neuronal networks, optimization algorithms.